Properties of Propagating Waves in Corona

Department of physics, SPPU

Project Guide: Dr. Girjesh Gupta, IUCAA

Monika Gundecha

May 2017

Aknowledgement

I would like to acknowledge my guide **Dr. Girjesh Gupta (IUCAA)** for the help and guidance I have received during my Masters project at **Dept. of Physics, Savitribai Phule Pune University(SPPU), Pune**, . I would also like to acknowledge **Inter University Center for Astronomy and Astrophysics(IUCAA), Pune** for providing me with all the necessary infrastructure and a conducive workplace to pursue the project. Finally, I would like to acknowledge my external project guide **Dr. Surjit Paul,Dept. of Physics,SPPU** for all the necessary collaboration.I would also like to thank Aishwanya for helping with the data,friends and family members for their constant support

Place: Pune, India
Date : 2^{nd} May,2017

Monika Sunil Gundecha

.

Contents

.

Chapter 1

Intorduction

1.1 Sun

Sun, the nearest star to Earth has been a part of research for many centuries. For an astronomer it is the only star that can be observed in great detail and, of course, its existence and properties are critical to us on Earth. The Sun is a very complicated object exhibiting highly variable and complex activity that cannot be simulated in laboratories and even the most powerful computers are still far away from the capacity of a detailed modeling of the largely variable parameter ranges from the hot interior of the Sun to its cool surface and again to the hot corona. It is a nearly perfect sphere of hot plasma, with internal convective motion that generates a magnetic field via a dynamo process. It is by far the most important source of energy for life on Earth. About three quarters of solar mass consists of hydrogen and the rest is mostly helium, with much smaller quantities of heavier elements, including carbon, oxygen, neon, and iron.The sun is a G-type main sequence star based on its spectral class. The sun is roughly middle aged; it has not changed dramatically for more than four billion years and will remain fairly stable for more than five billion years.

Basic facts about the Sun:

Age = $4.5X10^9$ years

Mass= $1.99X10^30$kg

Radius= 6,96,000 km

Average density = 1408 kg/m^3

Average distance from the Earth (1 AU) = $150X10^9$km

Gravitational acceleration on surface = 274 m/s^2

Rotation period at equator = 26 days

Effective black body temperature = 5778 K

1.2 Structure of Sun

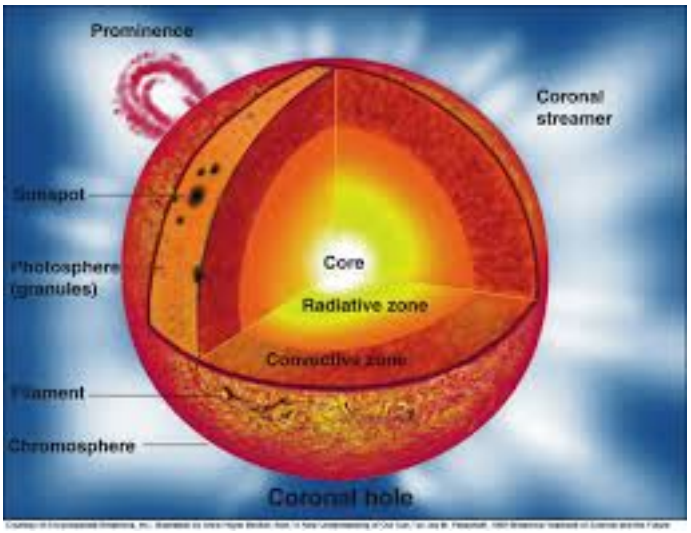

Figure 1.1: Structure of Sun,Courtesy:Anne Hoyer Becker,from 'A new understanding of Our sun',1989 Britannica yearbook of Science and Future

1.2.1 Core

The core of sun extends from the center to about 20-25% of the solar radius. It has a density of up to 150 g/cm^3 and a temperature of close to 15.7 million Kelvin. Energy which we receive from the sun is produced in it's core through nuclear fusion reaction which then transferred outwards through series of layers, finally to Photosphere where it escapes into space as Sunlight. Though most of the Sun's life, the energy has been produced by nuclear fusion in the core region through a series of steps called p-p chain. Only 0.8% of the energy generated in the Sun comes from CNO cycle, though this proportion is expected to increase as the sun becomes older.

1.2.2 Radiative Zone

This zone extends out from the core out to about 0.7 solar radii. The temperature drops from approximately 7 billion to 2 million Kelvin and density drops from 20g/cm^3 to 0.2g/cm^3 with increasing distance from the core. This temperature gradient is less than the value of adiabatic lapse rate, and hence cannot drive convection, which explains why the transfer of energy through this zone is by radiation instead of thermal convection. Photons take millions on years to cross this zone due to high density

1.2.3 Tacholine

The radiative zone and the connective zone are separated by a transition layer, the tachocline. Fluid motions found in the convection zone slowly disappear from top of this layer to its bottom where the conditions match those of calm radiative zone Presently it is hypothesized that a magnetic dynamo within this layer generates the sun's magnetic field.

1.2.4 Convective Zone

The sun's convection zone extends from 0.7 solar radii to near the surface. In this layer, the solar plasma is not dense enough or hot enough to transfer the heat energy of the interior via radiation. Instead, the density of plasma is low enough to allow convective currents to develop and move the sun's energy outward towards the surface. Material heated at the tachocline picks up heat and expands, thereby reducing its density and allowing it to rise. As a result, an orderly motion of the mass develops into thermal cells that carry the majority of the heat outward to sun's photosphere above. Once the material diffusively and radiatively cools just beneath the photospheric surface, its density increases, and it sinks to the base of the convection zone, where it again picks up heat from the top of the radiative zone and the convection cycle continues.

1.2.5 Photosphere

The visible surface of the Sun, the photosphere, is the layer below which the Sun becomes opaque to visible light. Above the photosphere visible sunlight is free to propagate into space. The photosphere is approximately 100km thick and is slightly less opaque than the lower part. An image of the Sun appears brighter in the center than on the edge or limb of the solar disk, in a phenomenon called as limb darkening. Temperature of this layer is approximately 6000 K.

1.2.6 Sun's Atmosphere

During a total solar eclipse, when the disk of the Sun is covered by that of the moon, the part of the Sun's surrounding atmosphere can be seen. It is composed of four distinct parts:

1. Chromosphere
2. Transition region
3. Corona
4. Heliosphere

The Chromosphere, transition region, and corona are much hotter than the surface of the Sun. The chromosphere is irregular layer above photosphere which is visible as a colored flash at the beginning and end of total solar eclipses. In this region temperature changes from 6000k to 20000k .Prominances and chromosheric networks are seen in this region. Above the chromosphere, in a thin transition region exists which separates hot corona from cooler chromosphere here, the temperature rises rapidly from around 20,000k to coronal temperatures closer to 100,000 k. Hydrogen is ionized at this stage so light is dominated by C iv, O iv, Si iv in UV region. The Corona is the next layer of the Sun. The average temperature of the corona and solar wind is about 1-2 million kelvin.The corona is extended atmosphere of the Sun which has a volume much larger than the volume enclosed by the Sun's photosphere. The heliosphere, the tenuous outermost atmosphere of the Sun.

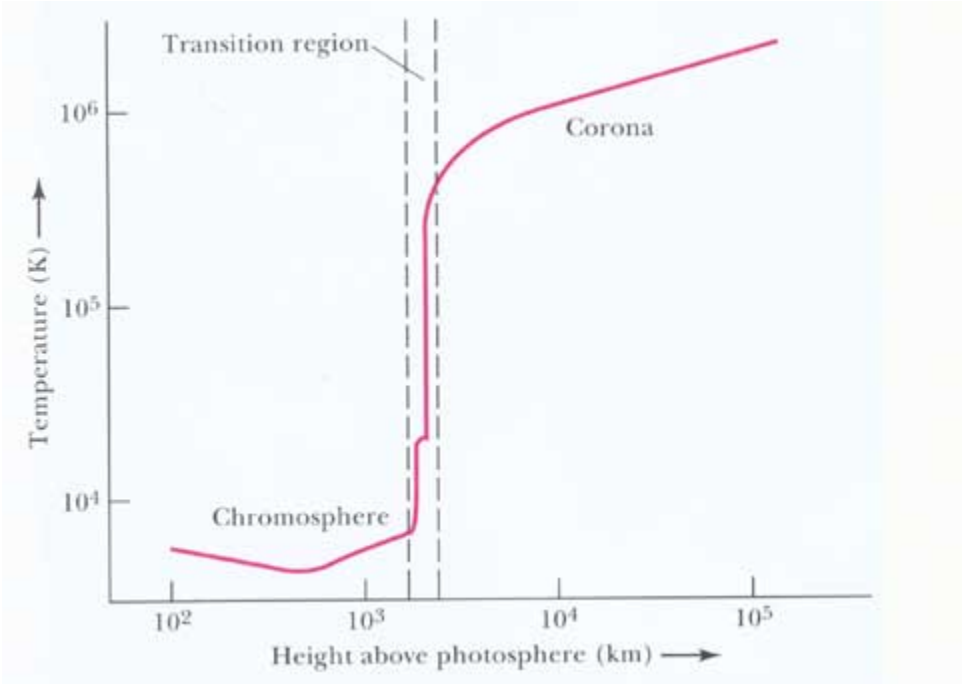

Figure 1.2: Temperature versus Height in solar atmosphere, Courtesy:Eugene Avrett, Smithsonian Astrophysical Observatory

As shown in the figure above temperature of the solar corona is very higher than photosphere.Heating of the corona thermally is not possible as it will violate second law of thermodynamics so the motivation behind this project is trying to study the possible mechanisms behind the heating problem such as wave theory.Study of solar corona will be done in following steps:

1.Identification wave guide

2.Study its time evolution

3.Identification of any wave signature

4.Find its period,frequency and speed

5.Look for different temperature filters

6.Compare speed in different temperatures

7.Variation in amplitude of oscillations with heights so find signature of wave damping and find its damping length

8.Find out fourier power index with height if any.

Chapter 2

Theory

2.1 Corona

Before moving on to the heating problem let's have a brief look at regions of corona.The Corona of Sun's atmosphere is subdivided into three zones, which all vary their size during the solar cycle: (1) Active regions, (2) Quiet Sun region, and (3) coronal holes.

Active regions

Like cities on the Earth globe, active regions on the solar surface harbor most of the activity, but make up only a small fraction of the total surface area. Active regions are located in areas of strong magnetic field concentrations, visible as sunspot groups in optical wavelengths or magnetograms. Sunspot groups typically exhibit a strongly concentrated leading magnetic polarity, followed by a more fragmented trailing group of opposite polarity. Because of this bipolar nature active regions are mainly made up of closed magnetic field lines. Due to the permanent magnetic activity in terms of magnetic flux emergence, flux cancellation, magnetic reconfigurations, and magnetic reconnection processes, a number of dynamic processes such as flares, and coronal mass ejections occur in active regions.

Quiet Sun

Historically, the remaining areas outside of active regions were dubbed quiet Sun regions. Today, however, many dynamic processes have been discovered all over the solar surface, so that the term quiet Sun is considered as a misnomer, only justified in relative terms. Dynamic processes in the quiet Sun range from small-scale phenomena such as network heating events, nanoflares, explosive events, bright points, and soft X-ray jets, to large-

scale structures, such as trans equatorial loops or coronal arches. The distinction between active regions and quiet Sun regions becomes more and more blurred because most of the large-scale structures that overarch quiet Sun regions are rooted in active regions. A good working definition is that quiet Sun regions encompass all closed magnetic field regions (excluding active regions), clearly demarcating the quiet Sun territory from coronal holes, which encompass open magnetic field regions.

Coronal holes

The northern and southern polar zones of the solar globe have generally been found to be darker than the equatorial zones during solar eclipses. Max Waldmeier thus coined those zones as Koronale Locher (in german, i.e., coronal holes). Today it is fairly clear that these zones are dominated by open magnetic field lines, that act as efficient conduits for flushing heated plasma from the corona into the solar wind, if there are any chromospheric upflows at their footpoints. Because of this efficient transport mechanism, coronal holes are empty of plasma most of the time, and thus appear much darker than the quiet Sun, where heated plasma upflowing from the chromosphere remains trapped until it cools down and precipitates back to the chromosphere.

2.2 Coronal Heating

In 1942, Bengt Edlén and Walter Grotrian identified Fe IX and Ca XIV lines in the solar spectrum (Edlén, 1943). From the formation temperature of these highly ionized atoms, a coronal temperature of T 1 MK was inferred for the first time. Comparing this coronal temperature with the photospheric temperature of 6000 K (4800 K in sunspots), we are confronted with the puzzle of how the 200 times hotter coronal temperature can be maintained, the so-called coronal heating problem. According to Second Law of Thermodynamics, the temperature in the corona should steadily drop down from the chromospheric value with increasing distance due to thermal conduction. Moreover, due to energy losses corona would just cool off within the duration of hours to days. Hence, to maintain the coronal plasma temperature to approximately 1 MK, a continuous source of heating is required. Now the question is how this non thermal energy is carried to and dissipated in solar corona

2.2.1 Heating Mechanisms

In general, any heating process is usually split into three phases: (i) the generation of energy; (ii) the transport of energy from the location of generation to solar atmosphere

(may be wave propagation); (iii) and mechanism for dissipation of energy in the atmosphere. However, there is a real difficulty in how the transported energy is dissipated efficiently on a time-scale so that the corona is not relaxed thermally. In most part of the solar atmosphere, plasma is embedded in magnetic fields. To describe these kind of system, a single unified framework, called Magneto-HydroDynamics (MHD) approach is more appropriate. As solar corona is highly dynamic and contains many different structures. Intuitively, it becomes obvious to visualize presence of waves in the solar atmosphere.While propagating, waves carry energy with themselves and can be dissipated in the medium in which they travel. These are the qualities which make MHD waves worthy for study in order to solve the coronal heating problem.

2.2.2 MHD Wave Heating

With increased spatial and time resolution it became possible to directly observe the wave and oscillatory processes in the solar atmosphere. In order to understand the various oscillations and waves in the solar atmosphere, a description of MHD equations and waves are necessary.Reproducing following MHD equations from Aschwanden,Physics of Solar Corona.

Ideal MHD equations

$$\frac{D}{Dt}\rho = -\rho \bigtriangledown .v \tag{2.1}$$

$$\rho\frac{DV}{Dt} = - \bigtriangledown P - \rho g + (j \times B) \tag{2.2}$$

$$\frac{D}{Dt}(P\rho^{-\gamma}) = 0 \tag{2.3}$$

$$\bigtriangledown \times B = 4\pi j \tag{2.4}$$

$$\bigtriangledown \times E = -\frac{1}{c}\frac{\partial B}{\partial t} \tag{2.5}$$

$$\bigtriangledown \cdot B = 0 \tag{2.6}$$

$$E = -\frac{1}{c}(v \times c) \tag{2.7}$$

Here ρ is plasma density, v is plasma fluid velocity, p is kinetic pressure, g is acceleration due to gravity, γ is ratio of specific heat, B is magnetic field, j is current density,E is electric field and,

$$\frac{D}{dt} = (\frac{\partial}{\partial t}) + v \cdot \bigtriangledown \tag{2.8}$$

signifies the total derivative.

Assuming that there exists equilibrium solution i.e

$$(\frac{\partial}{\partial t} = 0) \tag{2.9}$$

and no flows i.e

$$v_0 = 0 \tag{2.10}$$

sound speed is given as

$$C_s^2 = \frac{\gamma P}{\rho} \tag{2.11}$$

and introducing small perturbations

$$\rho(x,t) = \rho_0 + \rho_1(x,t) \tag{2.12}$$

$$v(x,t) = v_1(x,t) \tag{2.13}$$

$$B(x,t) = B_0 + B_1(x,t) \tag{2.14}$$

In the simplest concept we can consider the perturbation as local phenomenon and neglect large scale gradients of macroscopic parameters.Therefore we neglect -ρ_0g and take B_0,ρ_0 to be constant.The MHD equations then yield the dispersion relation for incompressible case,

$$v_A^2 = \frac{\omega^2}{k^2} \tag{2.15}$$

Where k is wave propagation vector, ω is angular frequency and v_A is associated Alfvén speed given by,

$$v_A = \frac{B_0}{\sqrt{4\pi\rho_0}} \tag{2.16}$$

Due to incompressible nature, no density or pressure changes are associated with it. This incompressible wave is called a shear Alfvén wave and falls into the category of transverse waves.Alfvén waves are driven by magnetic tension force alone and propagates along the magnetic field. For compressible case, above described plasma will lead to the dispersion relation,

$$\omega^4 - k^2(C_s^2 + v_A^2)\omega^2 + k_z^2 k^2 C_s^2 v_A^2 = 0 \tag{2.17}$$

Where wave propagation vector $\mathbf{k} = (k_x, k_y, k_z)$ has an absolute value of $k = |\mathbf{k}| = (k^2x + k^2y + k^2z)$ The cosine of the wave vector in the direction to the magnetic field is k_Z, so the propagation angle θ is

$$\cos\theta = \frac{k_z}{k} \tag{2.18}$$

Introduction of compressibility do not change the Alfvén wave mode, but leads to the additional two wave modes called as fast and slow magneto-acoustic waves. Dividing the dispersion relation (Equation 2.17) by k^4, it can be expressed as a function of the phase speed v_ph and propagation angle θ,

$$v_(ph)^4 - v_(ph)^2(C_s^2 + v_a^2) + C_s^2 v_A^2 \cos^2\theta \tag{2.19}$$

Using this equation, phase speed diagram $V_(ph)(\theta)$ is shown as polar plot in Figure 2.1. It can be seen that the slow mode has a phase speed in the range of $0 \leqslant v_(ph) \leqslant min(C_s, V_A)$, having a maximum for propagation along the magnetic field and cannot propagate perpendicularly to the magnetic field. Whereas the fast mode has a phase speed in the range of $max(C_S, v_A) \leqslant V_(ph) \leqslant \sqrt{(C_S^2 + v_A^2)}$, with the fastest mode propagating perpendicularly to the magnetic field.

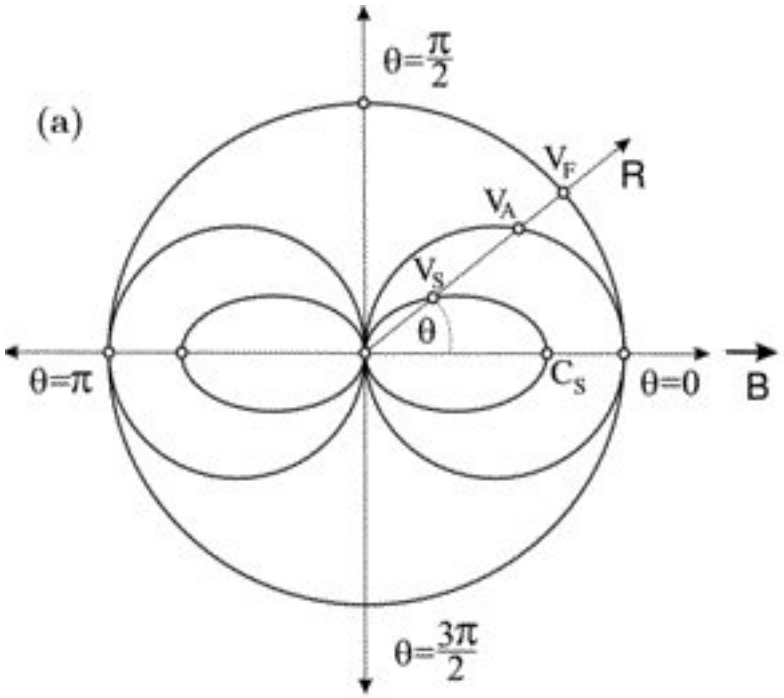

Figure 2.1: Polar diagram showing MHD waves courtesy:Linden et al, 2009

Chapter 3

Observational Data

3.1 Obtaining the data

Studying astronomy from the Earth's surface is limited by the filtering and distortion of electromagnetic radiation due to the Earth's atmosphere.A telescope orbiting the Earth outside the atmosphere will not be affected by twinkling and light pollution from artificial light sources on the Earth.Space based astronomy is even more important for frequency ranges which are outside the optical and radio window,as they are severely attenuated by atmosphere.Therefore to observe the Universe in different part of electromagnetic spectrum telescopes are sent into the space.The Sun's atmosphere which plays an important role in Space Weather, is extremely hot,more than a million degree. Such high temperature gas emits high energy radiation known as Extreme Ultraviolet (EUV) and X-ray radiation. EUV and X-rays are used to view the Sun's corona since they allow us to differentiate the hot and cold parts of the Sun. By imaging the Sun from space at these wavelengths, heating mechanisms of these gases can be understood along with its effect on the Earth and its space environment.To study solar phenomena data is obtained from various observatories like SOHO, TRACE and Hinode, SDO. For this project data from SDO (Solar Dynamics Observatory) is used.

3.1.1 Solar Dynamic Observatory

The Solar Dynamics Observatory (SDO) is the first mission to be launched under NASA's Living With a Star (LWS) program. This program involves a diverse set of research topics that aim to provide a greater understanding how the activity and variability of the Sun affect life on Earth. The purpose of SDO is to understand how the Sun's magnetic field is generated and structured, and how this stored magnetic energy is converted and released into the helio-

sphere and geospace in the form of solar wind, energetic particles, and variations in the solar irradiance. SDO was launched aboard an Atlas V rocket on 11 February 2010 from Kennedy Space Center in Florida. It is now located in a nearly geosynchronous orbit that allows continuous contact with its dedicated ground stations in New Mexico. The observatory has more or less been operating nominally since launch, without any major problems.

The observatory contains three instruments:

The Atmospheric Imaging Assembly (AIA) is an array of 4 telescopes that together provide full-disk images of the solar corona at 1 resolution (4096×4096-pixel images) in 10 UV and EUV wavelengths every 10 seconds;

The Extreme ultraviolet Variability Explorer (EVE) measures the EUV spectral irradiance with unprecedented spectral resolution, temporal cadence, accuracy, and precision; and

The Helioseismic and Magnetic Imager (HMI) provides full-disk, high-cadence Doppler, intensity, and magnetic images at 1 resolution (4096×4096-pixel images) of the solar photosphere, allowing studies of the sources and evolution of activity within the solar interior.

3.1.2 Atmospheric Imaging Assembly (AIA)

: Seven EUV and three UV-visible channels. Four of the EUV wavelength bands open new perspectives on the solar corona, having never been imaged or imaged only during brief rocket flights. The set of six EUV channels that observe ionized iron allow the construction of relatively narrow-band temperature maps of the solar corona from below 1 MK to above 20 MK. A field of view exceeding 41 arcmin (1.28 solar radii in the EW and NS directions), with 0.6 arcsec pixels with temporal resolution of 12s Table for different wavelength bands is given below:

Channel name	Primary ion(s)	Region of atmosphere*	Char. log(T)
white light	continuum	photosphere	3.7
1700Å	continuum	temperature minimum, photosphere	3.7
304Å**	He II	chromosphere, transition region	4.7
1600Å**	C IV+cont.	transition region + upper photosphere	5.0
171Å**	Fe IX	quiet corona, upper transition region	5.8
193Å**	Fe XII, XXIV	corona and hot flare plasma	6.1, 7.3
211Å**	Fe XIV	active-region corona	6.3
335Å**	Fe XVI	active-region corona	6.4
94Å**	Fe XVIII	flaring regions (partial readout possible)	6.8
131Å**	Fe VIII, XX, XXIII	flaring regions (partial readout possible)	5.6, 7.0, 7.2

Figure 3.1: Different wavelegth bands in AIA, Courtesy:https://aia.lmsal.com/index.htm

SDO data can be browsed through these web pages: “The Sun Now” , “Sun In Time”, SolarMonitor and Helioviewer and JHelioviewer.Request for the particular data can be made on the page http://www.lmsal.com/get_aia_data/

3.1.3 software

Data analysis was done using the SolarSoft system which is a set of integrated software libraries, data bases, and system utilities which provide a common programming and data analysis environment for Solar Physics It is primarily an IDL based system.IDL stands for Interactive Data Language.

3.2 Data Analysis

We chose 45 minutes in time sequence in 171$\mathring{A}$, 191$\mathring{A}$ and 211$\mathring{A}$ passbands on 11 Dec 2010 from 09:30am to 10:14am.Data contains 225 time frames with 12s cadence.All the images are calibrated,coaligned and rescaled to 0.6” frame.

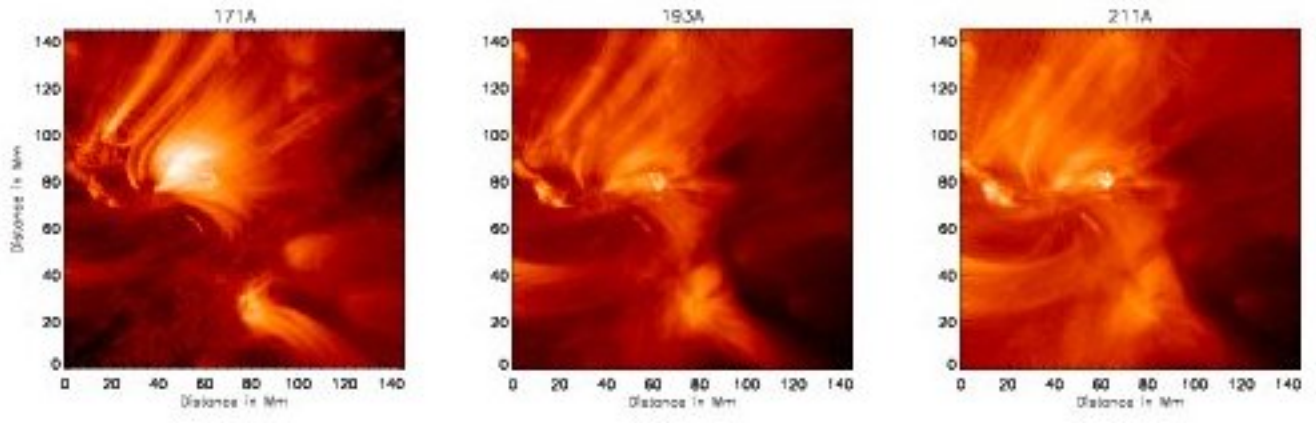

Figure 3.2: Images in different pass filters taken on 11 DEC, 2010 at 10:05 am UT

From this data two different slits along the loops coming out around the sunspot are choosen.Slit A is a array of dimension (23,225) which covers distance of 10 Mm above the surface of the sun.Where as slit B is array of dimension (29,225) covering 12 Mm distance above the surface of the sun.These slits are shown in fig 3.3

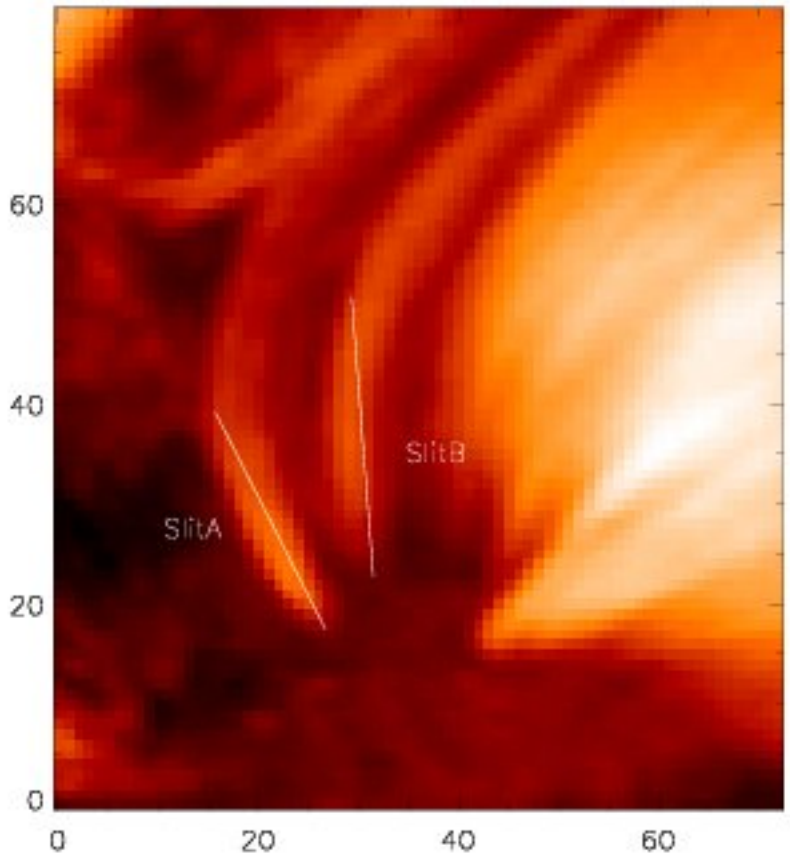

Figure 3.3: Slit A and Slit B along the loops in 171 $\AA$ taken on 11 Dec 2010 at 10:05 UT

Chapter 4

Results and Discussion

Processed time-distance intensity maps for slits marked in fig 3.3 are plotted as shown in fig4.1 and fig 4.2.From the figure, signatures of propagating ridges can be clearly seen.From the slope of these propagating ridges we found speed of propagation of waves.These speeds measured were different in different pass bands.For slit A propagation speed were approximately 17 km/s, 18 km/s and 19km/s for 171 $\mathring{A}$,193 $\mathring{A}$ and 211 $\mathring{A}$ respectively.Ratio of propagating speed between 193$\mathring{A}$ and 171$\mathring{A}$ is 1.05.For slit B propagation speed were approximately 24 km/s, 27 km/s and 25km/s for 171$\mathring{A}$, 193$\mathring{A}$ and 211$\mathring{A}$ respectively.Ratio of propagating speed between 193$\mathring{A}$ and 171$\mathring{A}$ is 1.12.whereas the ratio of peak temperature of dominant contributing ions between these two filters can be anywhere in the range 1-1.58-1.99-2.24.(Dominant ion contributing in 171$\mathring{A}$ is Fe IX where as in 193 $\mathring{A}$ are Fe Ix,Fe X,Fe XI,Fe XII)These ratios are close enough to follow relation of acoustic waves $C_s \propto \sqrt{T}$ ref(eq. 2.11).It can be seen that speed of these disturbances increases with temperature.Hence,propagating disturbances can be attributed to the presence of propagating slow magneto-acoustic wave(from sec 2.2.2)s.

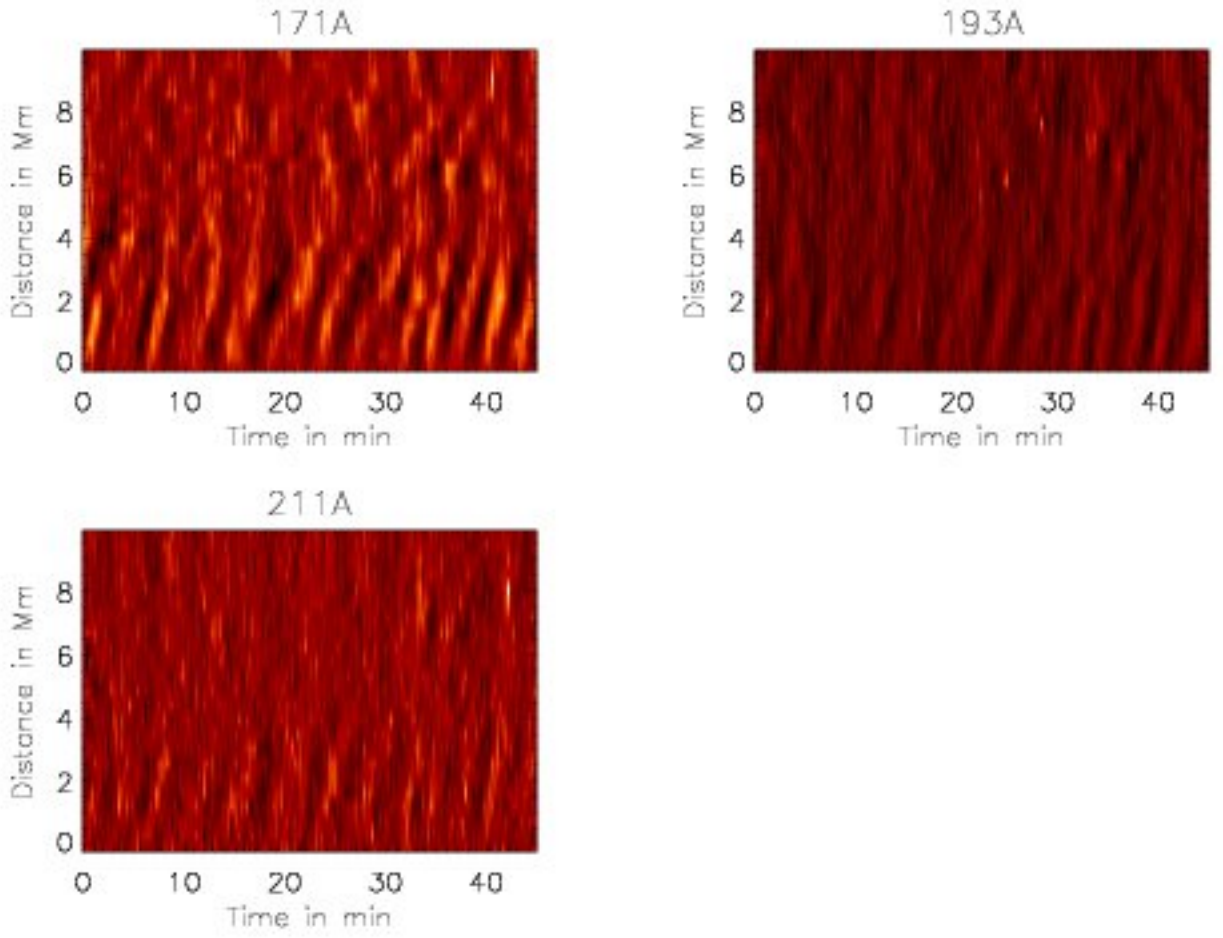

Figure 4.1: Distance Vs Time plot for slit A in all filters

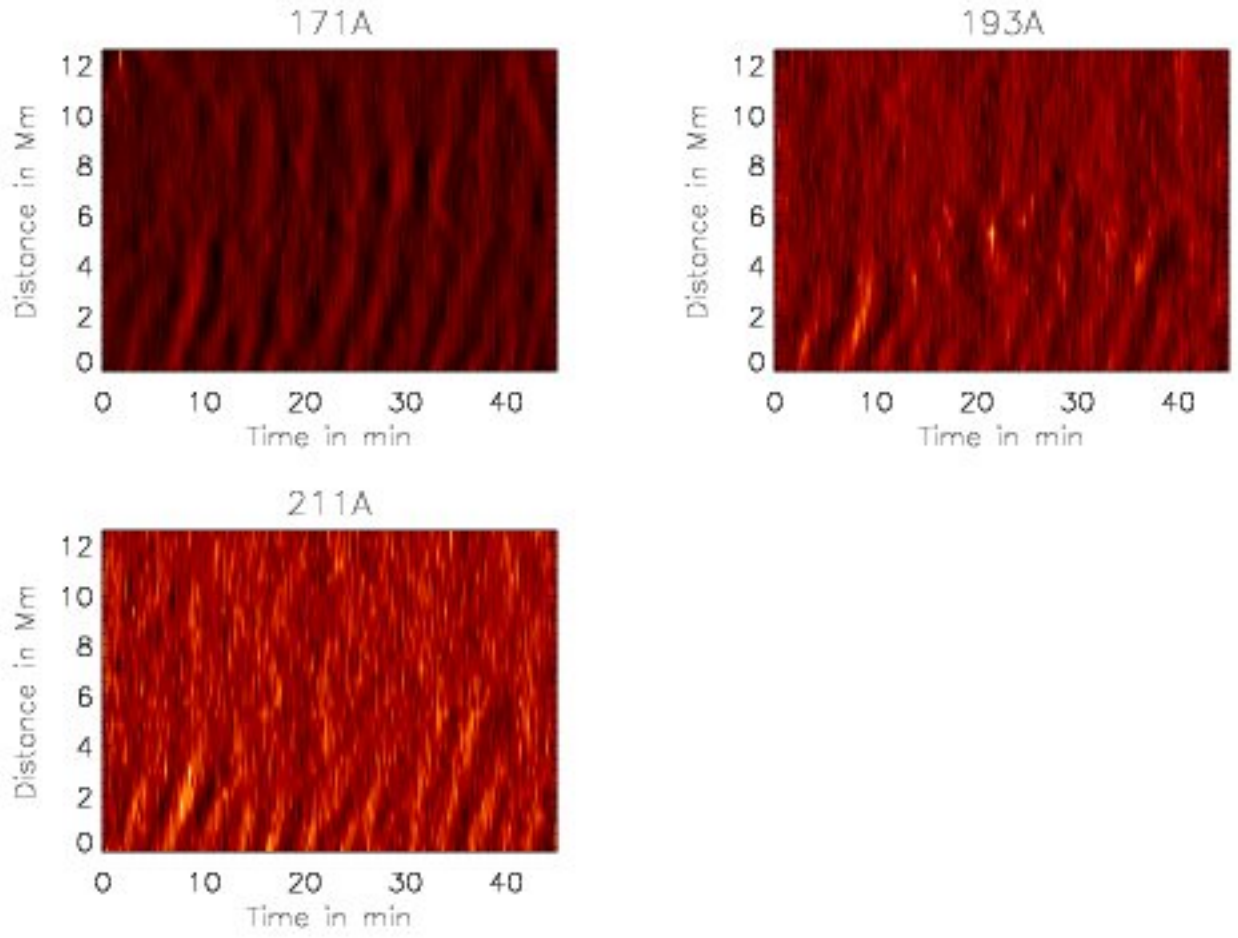

Figure 4.2: Distance Vs Time plot for slit B in all filters

Frequency-distance Fourier power map of propagating disturbances

The result presented above provides evidence of propagating slow magneto-acoustic waves.Data contains period ranges from 45 min to 1 min.Now we found fourier transform values with height in different frequency ranges.

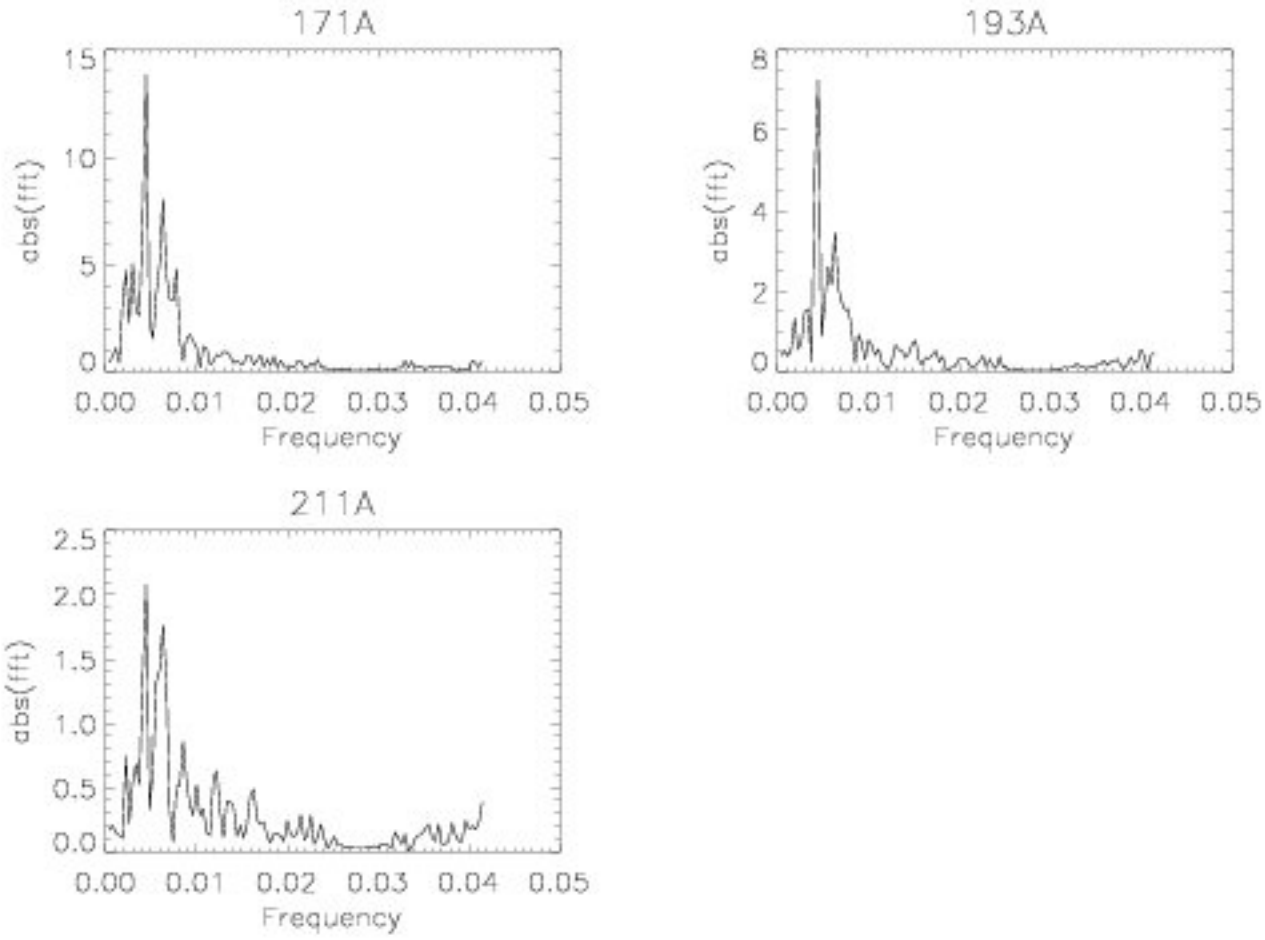

Figure 4.3: Fourier transform values with respect to frequencies at the height of 2.2Mm in 171$\mathring{A}$, 193$\mathring{A}$ and 211$\mathring{A}$ for slit A

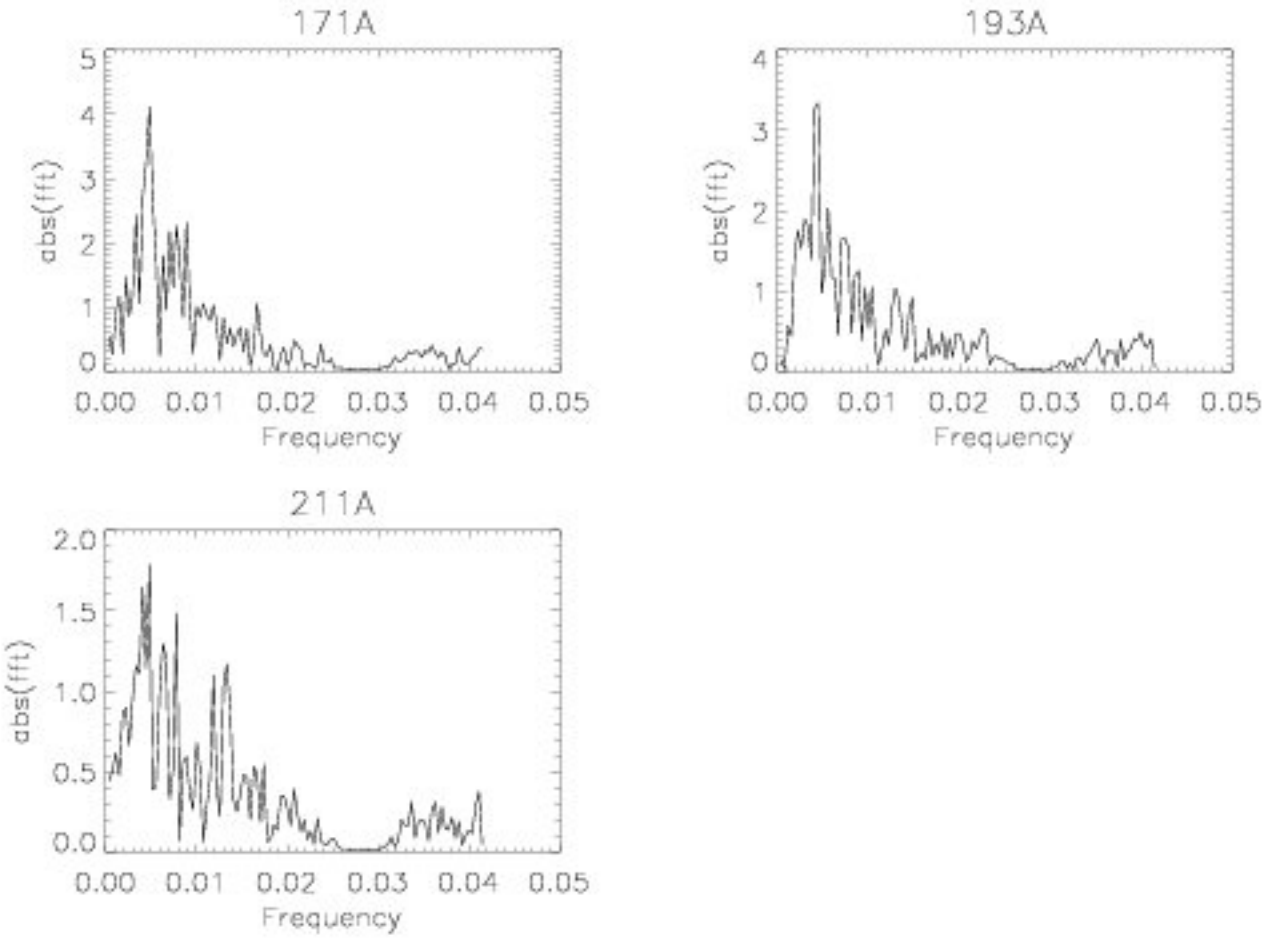

Figure 4.4: Fourier transform values with respect to frequencies at the height of 8.8Mm in 171$\mathring{A}$, 193$\mathring{A}$ and 211$\mathring{A}$ for slit A

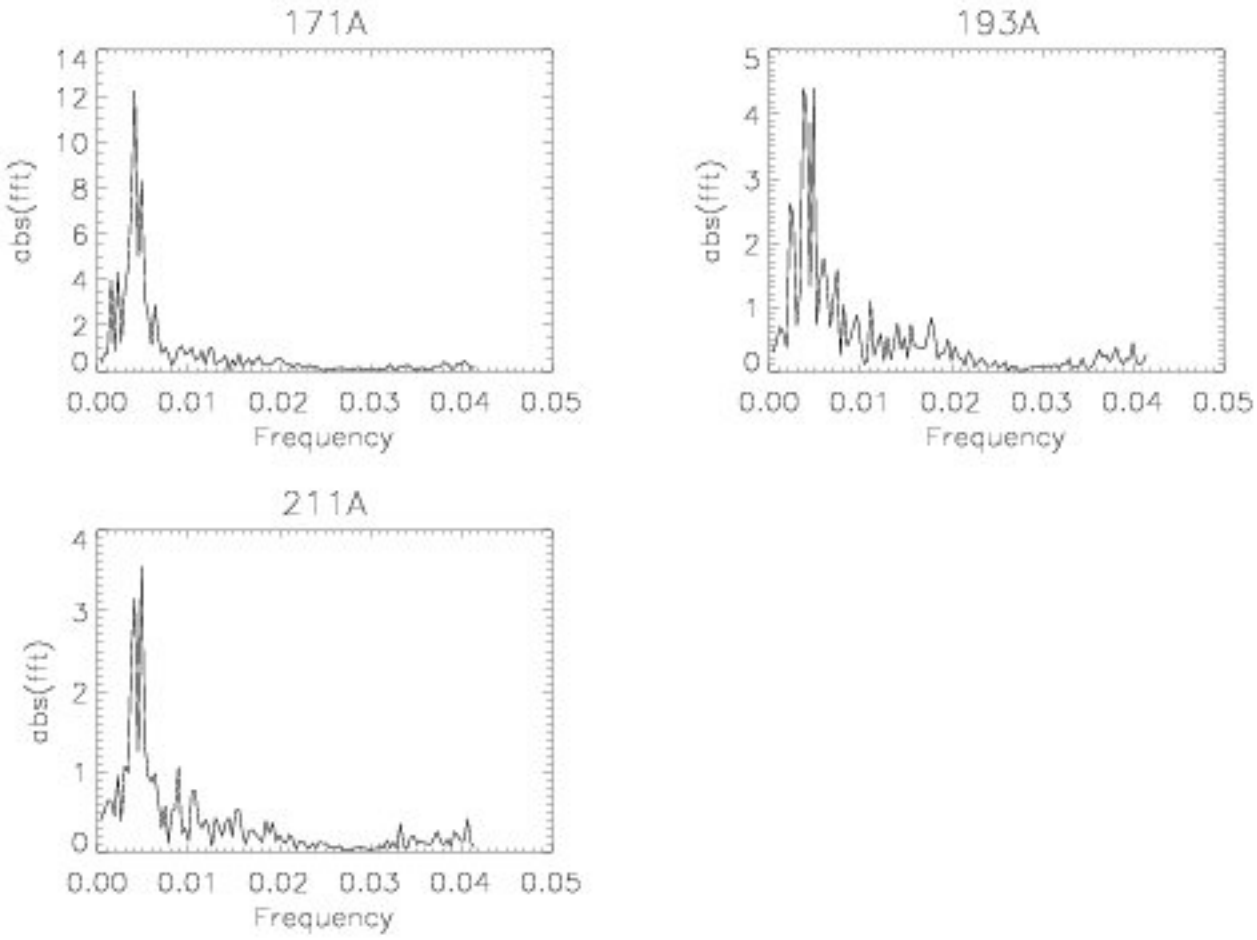

Figure 4.5: Fourier transform values with respect to frequencies at the height of 2.2Mm in 171$\mathring{A}$, 193$\mathring{A}$ and 211$\mathring{A}$ for slit B

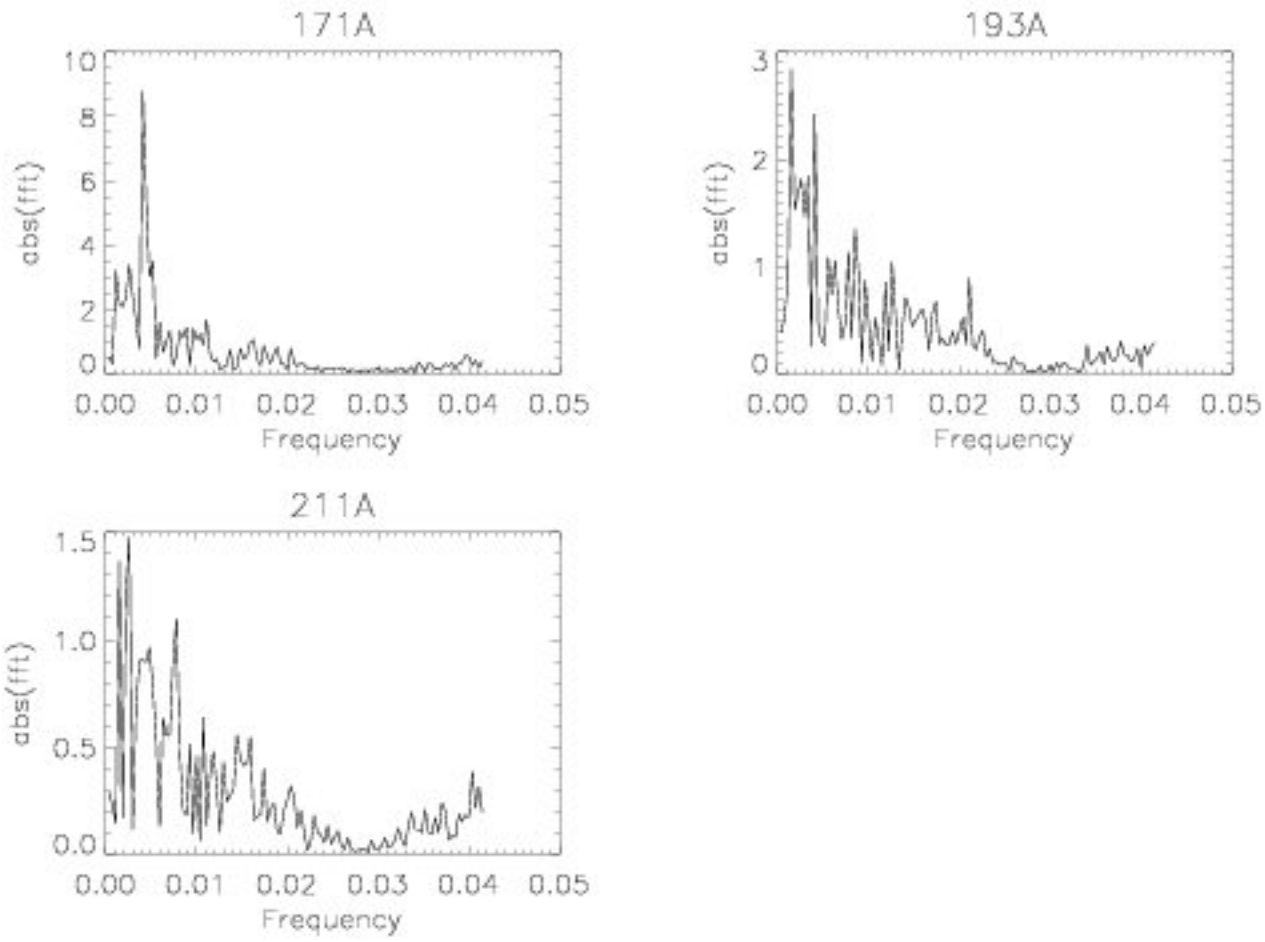

Figure 4.6: Fourier transform values with respect to frequencies at the height of 8.8Mm in 171$\mathring{A}$,193$\mathring{A}$ and 211$\mathring{A}$ for slit B

From Fourier Transform plots it can be seen that lower frequency hence the longer periods have higher FT values.These FT plot were obtained at 2.2Mm and 8.8Mm height for both the slits and it can be seen in above figures that with respect to increase in height the absolute value of fourier transform is decreasing showing possibility of wave damping.

Chapter 5

Future scope

In the result, decrease in FT vaues with respect height can be seen however this decrease in FT values with height can be due to gravitational stratification and area divergence which are geometrical effects and not due to actual wave dissipation.Both these effects combined together reduces FT values quickly with height and take form proportional to both.Expected decrease in FT values due gravitational stratification can be taken into account as follows.Following Ofman et al.(1999),equilibrium density in solar atmosphere is given as

$$\rho = \rho_0 \exp[-\frac{R_0}{H}(1 - \frac{R_0}{r})] \tag{5.1}$$

and approximate change in density due to wave propagation as

$$d\rho = \frac{R_0}{r} \exp[-\frac{R_0}{2H}(1 - \frac{R_0}{r})] \tag{5.2}$$

where R_0 is solar radius,H is density scale height and $r = R_0 + h$ (h is height above surface of sun) $I \propto \rho\Box$, thus change in due to wave propagation will be obtained as

$$dI \propto 2\rho d\rho \propto \frac{R_0}{r} \exp[-\frac{3R_0}{2H}(1 - \frac{R_0}{r})] \tag{5.3}$$

The of FT values obtained in different frequency ranges with respect to height can be compared with the expected decrease with height after taking the effect of gravitation and are of divergence into account as obtained in equation (5.3).This will help us to find decrease in FT values due to real dissipation of wave energy.Also we can study possible damping mechanism.Further we can find fourier power index with height($P_f \propto f^{-}\alpha$), if any from fourier power distribution.It may indicate presence of MHD turbulance which could be important in excitaton and damping of waves.

Bibliography

[1] Gupta,2014

[2] Ashwanden,Physics of Solar Corona,2004

[3] Arnab Raichoudhary,The Physics of Fluids and Plasmas

[4] Lemen et al.2012,The Atmospheric Imaging Assembly (AIA) on the Solar Dynamics Observatory (SDO)

[5] Ofman et al, 1999,Slow Magnetosonic Waves in Coronal Plumes

[6] Gumley,Practical IDL Programming

[7] SDO:https://www.lmsal.com/sdodocs/doc/dcur/SDOD0060.zip/zip/entry/

[8] AIA:https://aia.lmsal.com/index.htm

[9] structure of sun:https://solarscience.msfc.nasa.gov/corona.shtml

[10] Leon Golub,Solar Corona,2010

[11] Zirker et al,1993,Coronal Heating